Glycosyltransferase Function in Core 2-Type Protein O-Glycosylation

Erica L. Stone[1], Mohd Nazri Ismail[2], Seung Ho Lee[3], Ying Luu[4], Kevin Ramirez[1], Stuart M. Haslam[2], Samuel B. Ho[4], Anne Dell[2], Minoru Fukuda[3] and Jamey D. Marth[1*]

[1]Howard Hughes Medical Institute and the Department of Cellular and Molecular Medicine, University of California San Diego, La Jolla, California 92093

[2]Division of Molecular Biosciences, Faculty of Natural Sciences, Imperial College London, London, SW7 2AZ, UK

[3]Burnham Institute for Medical Research, La Jolla, California 92037

[4]Department of Medicine, VA San Diego Healthcare System and the University of California, San Diego, La Jolla, CA 92161

Running Title: Biology and Structure of Core 2 O-Glycans

Materials and Methods Word Count: 2,405

Combined Word Count Introduction, Results, Discussion: 3,990

[*]Proofs, reprints and correspondence should be addressed to Jamey D. Marth at 9500 Gilman Drive-0625, UCSD, La Jolla, CA., 92093; Tel: (858) 534-6526; Fax: (858) 534-6724; e-mail: jmarth@me.com

Abstract

Three glycosyltransferases have been identified in mammals that can initiate the biosynthesis of Core 2 type protein O-glycosylation. Core 2 O-glycans are abundant among glycoproteins but to date few functions for these structures have been identified. To investigate the biological roles of Core 2 O-glycans, we have generated and characterized mice deficient in one or more of the three known glycosyltransferases that generate Core 2 O-glycans (C2GnT1, C2GnT2, C2GnT3). A role for C2GnT1 in selectin ligand formation has been described. We now report that C2GnT2 deficiency impaired the mucosal barrier and increased susceptibility to colitis. C2GnT2 deficiency further resulted in the loss of all Core 4 O-glycan biosynthetic activity and reduced immunoglobulin abundance. In contrast, loss of C2GnT3 altered behavior linked to reduced Thyroxine levels in circulation. Remarkably, absence of all three C2GnTs was permissive of viability and fertility. Core 2 O-glycan structures were reduced among tissues from individual C2GnT deficiencies and completely absent from triply-deficient mice. C2GnT deficiency also induced alterations in I-branching, Core 1 O-glycan formation and O-mannosylation. Although the absence of C2GnT and C4GnT activities is tolerable *in vivo*, Core 2 O-glycosylation exerts a significant influence on O-glycan biosynthesis and is important in multiple physiological processes.

Introduction

Protein O-glycosylation is a posttranslational modification implicated in a wide range of physiological processes including: cell adhesion and trafficking, T-cell apoptosis, cell signaling, endocytosis and pathogen-host interaction (1, 6, 27, 30, 54, 61, 71). Core-type protein O-glycosylation is initiated in the secretory pathway by the covalent addition of a *N*-acetylgalactosamine (GalNAc) to the hydroxyl group of serine or threonine residues by one of multiple polypeptide N-acetylgalactosamine transferases (ppGalNAcTs) (57, 58). The ppGalNAcTs have differences in substrate specificity, with some ppGalNAcT acting preferentially on specific peptide sequences and others acting only after a GalNAc linkage has been formed nearby (20, 44). Following ppGalNAcT action, other glycosyltransferases act, sequentially and sometimes competitively, to elaborate the repertoire of O-glycan structures (31, 42, 48, 49).

The Core 2 β1,6-*N*-acetylglucosaminyltransferases (C2GnTs) and the Core 2 O-glycans they generate are conserved and widely expressed among mammalian species. The C2GnTs operate after Core 1 β-1,3-galactosyltransferase, which adds a galactose in a β1,3-linkage to the GalNAc-Ser/Thr generating the initial Core 1 O-glycan disaccharide structure (26). One of the three C2GnTs (C2GnT1, C2GnT2 and C2GnT3) subsequently adds an *N*-acetylglucosamine (GlcNAc) in a β1,6-linkage to the GalNAc to initiate what is known as the Core 2 O-glycan branch (Figure 1a) (7, 50, 51, 69). In a distinct pathway, Core 3 β-1,3-*N*-acetylglucosaminyltransferase (C3GnT) can add a GlcNAc to the unmodified GalNAc to generate a Core 3 O-glycan (24). In this case, C2GnT2 can add a GlcNAc in β1,6-linkage to the GalNAc of the Core 3 O-glycan disaccharide to initiate formation of a Core 4 O-glycan (Figure 1b) (50, 69). In addition, both C2GnT2 and the I β-1,*6*-*N*- acetylglucosaminyltransferase (IGnT)

are independently capable of forming branched polylactosamine structures (I-branches) from otherwise linear polylactosamine glycan chains (Figure 1c) (69).

C2GnT1-deficient mice have been shown to have an unexpectedly restricted phenotype with the major defect being leukocytosis reflecting neutrophilia (14). This appears to be due to a selective and severe defect in selectin ligand biosynthesis among myeloid cells, leading to decreased recruitment of neutrophils that further attenuates inflammation and vascular disease pathogenesis (14, 64). C2GnT1-deficient mice also exhibit a partial reduction in L-selectin ligand biosynthesis on high endothelial venules (HEV), resulting in reduced B-cell homing and colonization of peripheral lymph nodes (18, 21). Furthermore, thymic progenitors from C2GnT1 deficient mice have a reduced ability to home to the thymus due to loss of P-selectin ligands on these cells (46). However, as of yet, the biological functions of C2GnT2 and C2GnT3 have not been investigated. To investigate why multiple glycosyltransferases capable of Core 2 O-glycan formation have been conserved, we have generated mice singly and multiply deficient in the three C2GnTs, and characterized the resulting physiology and alterations to the glycome.

Materials and Methods

Mice

Genomic clones isolated from the 129/SvJ mouse strain were used to construct targeting vectors for *Gcnt3,* encoding C2GnT2, and *Gcnt4*, encoding C2GnT3. To generate individual targeting vectors for each gene, the genomic clones and the pflox vector were digested with the appropriate restriction enzymes as indicated (Figure 2). Each genomic clone was then ligated into the pflox vector to generate the targeting vector for each gene. The targeting vectors were then individually electroporated into R1 ES cells (39). Homologous recombination between the

targeting vector and genomic DNA resulted in F[tk-neo] alleles. G418 (to select for neo gene expression) was used to select for cells in which the targeting vectors had integrated. A Cre-recombinase expressing plasmid was electroporated into these cells. Ganciclovir was used to select for colonies in which thymidine kinase (tk) was deleted by Cre-recombinase activity. Southern blotting of genomic DNA confirmed the expected allelic structures were present. Individual chimeric mice were obtained from C57BL/6NHsd blastocytes injected separately with ES cells containing the alleles in which the single coding exon of interest was flanked by loxP sites. Mice carrying these alleles, $Gcnt3^{F}$ or $Gcnt4^{F}$, in the germline were crossed with female ZP3-Cre mice to generate separate mice with systematic deletions, $Gcnt3^{\Delta/\Delta}$ or $Gcnt4^{\Delta/\Delta}$. Experimental mice were on a mixed background of 129Sv/J and C57BL/6NHsd for this reason littermate control mice were used when ever possible.

Crossing of single deficient strains generated mice deficient in multiple C2GnTs. C2GnT1-deficient mice, which have been previously described (14), were crossed to C2GnT3-deficient mice to generate mice heterozygous for both alleles. These doubly heterozygous mice were bred to each other to generate mice doubly deficient for C2GnT1 and C2GnT3 (T1/T3). T1/T3 mice were then bred to C2GnT2-deficient mice to generate mice heterozygous for all three genes encoding C2GnTs. Triply heterozygous mice were bred together to generate offspring doubly deficient for C2GnT1 and C2GnT2 (T1/T2) and doubly deficient for C2GnT2 and C2GnT3 (T2/T3) as well as mice deficient for all three C2GnTs (T1/T2/T3). Some T1/T2/T3 mice were used in additional breedings to generate experimental mice. Animal studies were accomplished in accordance with Institution Animal Care and Use Committee, University of California, San Diego.

Quantitative-PCR

RNA was obtained from wild-type C57BL/6NHsd mice. Tissues were harvested and stored at -80˚C. To isolate the RNA the tissue was placed in TRI-Reagent (Sigma, St. Louis, MO) and homogenized, after homogenization chloroform (Sigma, St. Louis, MO) was added for extraction. RNA was pelleted using isopropanol (Sigma, St. Louis, MO) and cleaned using 70% ethanol. RNA was dissolved in H_2O and treated with Turbo DNA-free (Ambion, Austin, TX) to remove DNA. RNA was run on an agarose-formaldehyde gel to determine quality and stored at -80˚C. RNA was quantified using OD_{260} and diluted to 0.5 μg/μl. qPCR was done as previously described with slight modifications (36). cDNA was generated using 1 μg of RNA and Superscript III First Strand (Invitrogen, Carlsbad, CA). cDNA product was diluted 1/10 in H_2O, and 1 μl of diluted cDNA plus 0.5 μm primers was used with Brilliant SYBR Green (Stratagene, Cedar Creek, TX) for the qPCR reaction. AGGCTCCTCTTCCCTCAAAG was used for the *Gcnt4* forward primer and ACATCACCGTCCTCCAAGTC as the *Gcnt4* reverse primer. Results were standardized using β-actin.

Selectin ligand expression

Selectin ligand expression was analyzed as previously described with slight modification (14, 59). Chimeras consisting of the lectin domains of mouse E- or P-selectin and the Fc portion of human IgG (R&D Systems, Minneapolis, MN) were bound to FITC-conjugated anti-human IgG antibody (Fc specific) (Sigma, St. Louis, MO) in binding media consisting of DMEM (Gibco) plus 2% IgG-Free BSA (Jackson ImmunoResearch, West Grove, PA) plus 2 mM $CaCl_2$ or 5 mM EDTA, and places in the dark at 4˚C for 30 minutes. White blood cells were washed with binding media and then stained with selectin-Fc chimeras prebound to anti-human Fc-FITC.

Selectin chimera binding to white blood cells was determined by flow cytometry using FACSCalibur System (BD Biosciences, San Jose, CA).

To activate T-cells, splenocytes were cultured in RPMI media plus 10% bovine serum in the presence of plate bound anti-CD3 (BD Biosciences, San Jose, CA) and 20 ng/ml IL-2 (R&D Systems, Minneapolis, MN) for 48 hours. At the indicated time points, cells were suspended in binding media and expression of activation markers or selectin ligands was determined by flow cytometry.

Hematology

Hematological parameters were determined utilizing a Hemavet 850FS (Drew Scientific, Wayne, PA) as previously described (59).

In vivo mucosal permeability assay

Mucosal barrier function was determined as previously described (17). Dextran-FITC (Sigma, St. Louis, MO) was administered via oral gavage (600 mg/kg) and blood was collected into Microtainer serum separator tubes (BD, Franklin Lakes, NJ) by retro-orbital bleeds at 4 hours. Blood was spun down in a tabletop centrifuge at 16.1 x *g* for 3 min to separate sera. The amount of FITC in each sample was measured in duplicate using Spectra Max Gemini EM fluorescent plate reader (Molecular Devices) at 490 nm and 530 nm for excitation and emission wavelengths, respectively.

DSS-induced colitis

Mice were administered drinking water containing 5% DSS (M.W. 40,000 to 50,000; USB Corporation, Cleveland, OH) *ad libitum* and then returned to normal drinking water without DSS. DSS was administered for 5 or 6 days. Occult or overt blood in the stool, stool consistency, weight and the activity level of the mice were determined daily through out the experiment and used to calculate disease activity index (DAI) as previously described (22). Mice surviving to the end of the experiment were then sacrificed, and colons were fixed in 10% buffered formalin for histological analyses. The amount of 5% DSS ingested was monitored daily and did not differ between groups. Mice that did not drink enough to surpass a DSS-load of 30mg/day were excluded from the study. Colon sections were stained with hematoxylin and eosin (H&E). The severity of mucosal injury was graded similarly to that described previously by (38, 40). Briefly, H&E stained section were read in a blinded manner to determine length of colon ulceration and crypt damage score. The injury scale was graded from 0 to III, as follows: grade 0: normal; grade I: distortion and/or destruction of the bottom third of glands; grade II: erosions/destruction of all glands or the bottom two thirds of glands and inflammatory infiltrate with preserved surface epithelium; and grade III: loss of entire glands and surface epithelium. Results are reported as total length of complete ulceration (grade III damage) and total crypt damage score as described (22).

Mucosal protein assays

A solution containing proteins from the mucosal layer was produced as described with slight modification (13). Feces were collected in a clean, empty cage for one hour. The feces

were weighed, diluted 20 fold weight to volume in phosphate buffered saline (PBS), and vortexed to make a fecal solution.

Relative Muc2 levels were determined by ELISA. Maxisorp 96-well plates (Nunc, Rochester, NY) were coated overnight at 4˚C with fecal solution diluted 10-fold further with PBS. The plates were washed with PBS, blocked with PBS plus 2% IgG-free bovine serum albumin (BSA; Jackson ImmunoResearch, West Grove, PA) for 1 hour at 22˚C, and then washed PBS plus 0.05% Tween 20 (PBST; Fisher Scientific, Pittsburg, PA). Antibody to Muc2 antigen H-300 (Santa Cruz Biotechnology, Santa Cruz, CA) diluted to 0.2 μg/ml in PBS plus 2% BSA was then allowed to bind overnight at 4˚C. The plates were then washed and coated with the secondary antibody anti-rabbit conjugated to horseradish peroxidase (HRP; Vector Laboratories, Burlingame, CA) diluted 1/1000 in PBS plus 2% BSA. Tetramethylbenzidine (TMB; Sigma, St. Louis, MO) was used as a substrate, and the plates were analyzed at 650 nm using a Versa max plate reader (Molecular Devices; Sunnyvale,CA).

Immunoglobulin analyses

Flat bottom Maxisorp 96-well plates were coated with 5 ug/mL of anti-mouse isotype specific antibodies (IgM, IgG1, IgG2a, IgG2b, IgG3 and IgA; BD Biosciences, San Jose, CA) in PBS overnight at 4˚C. Plates were blocked with 2% BSA. Sera samples were diluted 1/2,000 (for IgG1, IgG2a and IgA) or 1/10,000 (for IgG3, IgM and IgG2b) in PBS plus 2% BSA and incubated for 2 hours at 22˚C. Fecal solutions were diluted 1/100 in PBS plus 2% BSA. Plates were washed with PBST. Alkaline phosphatase (AP)-conjugated antibodies to mouse IgG1, IgG2a, IgG2b, and IgG3 (BD Biosciences, San Jose, CA) were diluted 1/500 in PBS plus 2% BSA. AP-conjugated antibodies to mouse IgM (1/4000) and IgA (1/1000) were purchased from

Sigma (St. Louis, MO). Plates were incubated with these secondary antibodies for 1 hour at 22˚C, washed with PBST and then the AP substrate para-nitrophenyl phosphate (Sigma, St. Louis, MO) was added. Signals were determined at 405 nm on a Versa max plate reader.

Behavioral testing

Behavioral screening included gross physical assessment, analysis of sensorimotor reflexes and the following assays: acoustic startle, prepulse inhibition, hot plate, tail flick, conditioned fear, initiation of movement, rotarod, wire hang, grip strength, cage-top hang test and pole test. These tests were accomplished as previously reported (3, 28). In the tube test for social dominance mice of different genotypes are put into opposite ends of a 30 cm long tube (29). The mouse that stays in the tube and causes the other to back out is considered dominant and said to have "won" the challenge. If neither mouse backed out of the tube within 60 sec, the challenge was deemed a "tie." Each mouse was challenged three times against 3 different mice including littermates of the opposite genotype.

Determination of thyroid hormone levels

T4 levels were determined by T4 Enzyme Immunoassays (EIA; Monobind Inc., Lake Forest, CA). TSH levels were determined by a two-site chemiluminometric assay at Hillcrest Medical Center of UC San Diego Medical Center.

Thyroid powder supplemented diet

Chow was supplemented with 0.025% porcine thyroid powder (Sigma, St. Louis, MO) as previously described (34) with minor modifications. The Purina 5053 base diet supplemented

with 0.025% porcine thyroid powder was purchased from Purina Test Diet (Richmond, IN). Thyroid powder supplemented chow was fed to wild-type and C2GnT3-deficient mice for 2 weeks in a conventional vivarium. Mice were analyzed by the tube test for social dominance prior to and following diet supplementation. Additionally, sera were collected at both time points following the tube test for social dominance. Sera were stored at -20˚C until used to determine T4 levels.

TRH stimulation assay

Mice were stimulated with TRH as previously described (67) with minor modifications. Blood was obtained at time zero and then mice were immediately administered by intraperitoneal injection 5 μg/kg of TRH (Sigma, St. Louis, MO) dissolved in 100 μl of PBS. Blood was then collected into serum separator tubes (BD, Franklin Lakes, NJ) at 1 or 2 hours and places in a tabletop centrifuge at 16.1 x *g* for 3 min to separate sera. Sera were stored in fresh microfuge tubes at -20˚C until analyzed.

T4 half-life assay

NHS-LC-biotin (10mg/kg of body weight) (Pierce, Rockland, IL) was injected intravenously into mice to biotinylate circulating proteins as similarly described (19). Mice were then bled at time zero. Blood was collected at additional time points in serum separator tubes. Sera were stored at -20˚C until assayed. Glycine was added to sera to quench any additional NHS activity. Biotinylated T4 remaining was determined by ELISA. A flat bottom Maxisorp plate was coated overnight at 4˚C with anti-T4 antibody (Santa Cruz Biotechnology, Santa Cruz, CA) diluted 1/1000 in PSB. The plates were washed with PBS and then blocked overnight at

4˚C with PBS plus 2% BSA. Sera samples were incubated on the blocked plates for 1 hour at 22˚C, and the plates were then washed with PBST. Streptavidin-HRP (BD Biosciences, San Jose, CA) diluted 1/5000 in PBS plus 2% BSA was allowed to bind for 45 min at 22˚C. Plates were washed again, TMB substrate was added, and plates were read at 650 nm using a Versa max plate reader.

Enzyme activity assays

Tissues from freshly sacrificed mice were immediately frozen using dry ice and stored at -80˚C until used. C2GnT and C4GnT activities from tissue lysates were determined as previously described (69).

Sample preparation for mass spectrometric analysis

Murine tissues were prepared for glycomic screening according to methodology described previously (56). Briefly, murine tissues were homogenized with Tris buffer and sequentially digested with trypsin (Sigma-Aldrich, Dorset, UK) and PNGase F (Roche, West Sussex, UK). N-glycans were separated from peptides/ glycopeptides on Sep-Pak cartridges (Waters, Hertfordshire, UK) and O-glycans were released from the latter by reductive elimination using KBH_4 in KOH. To optimize O-glycan extraction from mucinous tissues, especially stomach, the following modifications have been applied on the previous procedure. Stomach samples were homogenized with water and then glycolipids were extracted out with methanol and chloroform. After trypsin digestion, O-glycans were released from the glycopeptide/peptide pool without N-glycan removal. Although trace amounts of N-glycans

might be released together with O-glycans, this strategy enables an improved recovery of O-glycans.

After purification on Dowex columns (Sigma-Aldrich, UK), the O-glycan samples were permethylated and then further purified with Sep-Pak cartridges. O-glycans were eluted in aqueous acetonitrile fractions and then lyophilized. Glycans are normally eluted in the 35% and 50% acetonitrile fractions, therefore only these fractions were subjected to mass spectrometric analysis. All murine tissues were analyzed in duplicates or triplicates.

Mass spectrometric data acquisition

Permethylated samples were dissolved in 10 µl of methanol. Then 1 µl of dissolved sample was pre-mixed with 1 µl of matrix (20 mg/ml 2,5-dihydroxybenzoic acid (DHB) in 70% (v/v) aqueous methanol) and spotted onto a target plate. Matrix-assisted laser desorption/ionization (MALDI) mass spectrometric and tandem mass spectrometric (MS/MS) data were acquired on a 4800 MALDI-TOF/TOF mass spectrometer (Applied Biosystems) in the reflectron mode. The potential difference between the source acceleration voltage and the collision cell was set to 1 kV and argon was used as collision gas. The 4700 Calibration Standard kit, calmix (Applied Biosystems), was used as the external calibrant for the MS mode and [Glu1]fibrinopeptide B human (Sigma-Aldrich, UK) was used as an external calibrant for the MS/MS mode.

Comparison of the relative abundance of O-glycans between C2GnT2-deficient, C2GnT3-deficient and T1/T2/T3 mice with wild type mice of various tissues was done by comparing peak heights of molecular ions of similar masses and by comparing the total ion counts of the different classes of glycans.

Statistical analyses

Significance in the tube test for social dominance was determined by the chi-square test. For all other experiments the student's t-test was used to determine statistical significance.

Results

Expression of murine Gcnt3 and Gcnt4 RNA

Glycosyltransferases that generate Core 2 O-glycans are encoded by separate genes each with a single coding exon in the murine and human genomes. C2GnT1 is encoded by *Gcnt1*, C2GnT2 by *Gcnt3,* and C2GnT3 by *Gcnt4*. The numbering of the genes and the enzymes differ because the genes were named based on β1,6-GlcNAc transferase activity and the enzymes based on Core 2 activity. *Gcnt2* encodes IGnT, which has β-1,6-GlcNAc transferase activity but is not able to generate Core 2 O-glycans, as it is not able to act upon the Core 1 O-glycan as a substrate (32).

Analysis of relative expression of *Gcnt3* in adult wild-type C57Bl/6Nhsd mouse tissues by qPCR revealed that *Gcnt3* has high relative expression in the gastrointestinal tract, similar to the previously determined expression pattern of human *GCNT3* (69). Contrary to the expression of human *GCNT4* (51), relatively low levels of the mouse orthologue *Gcnt4* were found in the thymus. Our studies revealed highest levels of expression of murine *Gcnt4* in the small intestine, liver, and spleen (Figure 1b).

Germline deletion of Gcnt3 and Gcnt4

Gcnt3 and *Gcnt4* were targeted separately for deletion from the mouse germline. *Gcnt3* was targeted in embryonic stem (ES) cells using Cre-loxP conditional mutagenesis focused on

the single coding exon of *Gcnt3* (Figure 2a). ES cells in which loxP sites flanked the single coding exon of Gcnt3 were utilized to generate chimeric mice (Figure 2b). $Gcnt3^{F}$ mice were bred to mice expressing Cre-recombinase, under the control of the Zp3 promoter (52), to generate mice with a systematic deletion of *Gcnt3* ($Gcnt3^{\Delta}$). C2GnT2-deficient mice ($Gcnt3^{\Delta/\Delta}$) were viable, born at normal Mendelian ratios, and both genders were fertile.

The single coding exon of *Gcnt4* was similarly targeted using the Cre-loxP mutagenesis approach (Figure 2c). Chimeric mice were generated with ES cells that carried the $Gcnt4^{F}$ allele (Figure 2d). Breeding to Zp3-Cre mice was again utilized to produce offspring carrying the $Gcnt4^{\Delta}$ allele in the germline (Figure 2d). Both genders of mice homozygous for the $Gcnt4^{\Delta}$ allele were also born at expected Mendelian ratios without overt developmental abnormalities and exhibited normal fecundity as adults.

Hematology and selectin ligand biosynthesis in mice lacking either C2GnT2 or C2GnT3

As the selectin ligand biosynthesis defect in C2GnT1 deficient mice is incomplete, and as there is precedence for collaboration among glycosyltransferases in the biosynthesis of selectin ligands (35, 45), we analyzed mice lacking either C2GnT2 or C2GnT3 for signs of a selectin ligand defect. Hematological analyses revealed that C2GnT3-deficient mice ($Gcnt4^{\Delta/\Delta}$), but not C2GnT2-deficient mice, exhibited slight, but significant neutrophilia. No other alterations in hematological profiles were evident in mice singly deficient for C2GnT2 or C2GnT3 (Figure 3a). Additionally, no overt differences were observed in the cellularity of various immune tissues including in the peripheral lymph nodes, or in the expression of various markers on immune cells including B220 (data not shown). To determine if the neutrophilia exhibited by C2GnT3-deficient mice is a result of reduced selectin ligand biosynthesis in the absence of C2GnT3,

selectin ligand expression on neutrophils from C2GnT3-deficient mice was analyzed. Using flow cytometric measurements, neutrophils from these mice expressed unaltered P- and E-selectin ligands (Figure 3b). C2GnT2-deficient neutrophils also normally expressed ligands for P- and E-selectins (Figure 3c). In addition, the homeostasis of thymocytes within C2GnT3-deficient mice was unaltered (Figure 3d). C2GnT3-deficient thymocytes also exhibited normal expression of cell surface markers including 1B11, which is partly dependent upon Core 2 O-glycosylation (8) (Figure 3e). As selectin ligand expression is upregulated by activated T-cells and C2GnT3 is expressed in activated T-cells (36), we analyzed the expression of selectin ligands on activated C2GnT3-deficient T-cells. Upon stimulation with plate bound anti-CD3 antibody in the presence of IL-2, C2GnT3-deficient T-cells upregulated activation markers including CD69 and 1B11 similarly to activated wild-type T-cells (Figure 3f). Selectin ligand expression, as determined by cytometry, was also unaltered among these activated T-cells, revealing that C2GnT3 is not required for upregulation of selectin ligands under these conditions.

C2GnT2 deficiency impairs mucosal barrier function and increases pathogenesis of experimental colitis

As *Gcnt3* is relatively highly expressed in tissues with high epithelial cell content, we suspected that the gastrointestinal tract might be affected in C2GnT2 deficiency. In fact, C2GnT2-deficient mice, but not C2GnT3-deficient mice, were found to have increased mucosal permeability indicating a defect in the mucosal barrier (Figure 4a and data not shown). To test the ability of the gastrointestinal tract of C2GnT2-deficient mice to protect from chemically induced colitis, we used dextran sodium sulfate (DSS) to experimentally induce disease (22). There was a trend towards increased weight loss in C2GnT2-deficient mice treated with DSS

(Figure 4b). Also, on at least one day during each separate experiment the disease activity score for C2GnT2-deficient mice was significantly worse than for similarly treated wild-type counterparts (Figure 4c). At the end of the experiment, H&E stained colon sections were used to determine length and grade of ulceration in these tissues. DSS-treated C2GnT2-deficient mice exhibited significantly more colon damage with increased ulceration and increased damage to the crypts in the colon (Figure 4d, 4e and 4f).

Mucins, glycoproteins that derive a majority of their molecular weight from O-glycans, have been implicated in mucosal barrier function and protection from DSS-induced colitis (47, 60). However, the expression of Muc2, the major secretory mucin in the colon, is not reduced among mice deficient in C2GnT2 (Figure 4g).

Immunoglobulin deficiencies in the absence of C2GnT2

Levels of IgG1, IgG2a, and IgG2b were significantly reduced in the serum of C2GnT2-deficient mice (Figure 5a). There is also a trend towards decreased serum levels of IgG3 and IgA. In contrast to circulating IgA, mucosal IgA abundance was significantly decreased in C2GnT2-deficient mice (Figure 5b). Altered mucosal immune homeostasis, including the absence of mucosal immunoglobulins, has previously been associated with susceptibility to DSS-induced colitis (9, 37). Absence of C2GnT2 results in a defect in the immune system, characterized by a reduction in immunoglobulin levels that may be associated with an increase in disease susceptibility.

C2GnT3-deficient mice exhibit a behavioral abnormality linked to reduced Thyroxine levels

Increased fighting was observed between male mice in litters containing at least one C2GnT3-deficient animal, but not among litters that included C2GnT2-deficient mice. The behavior of male mice lacking C2GnT3 was further analyzed. C2GnT3-deficient male mice exhibited a significant increase in social dominance compared to wild-type male littermates (Figure 6a). This assay is often used as a measure of aggression (10). Hypothyroidism is one cause of aggression in mammals including dogs and horses (4, 12, 15, 62). Further phenotype screening revealed that C2GnT3-deficient mice had a slight but significant decrease of circulating Thyroxine (T4) levels (Figure 6b). To determine if the altered behavior observed in C2GnT3 deficiency was a result of insufficient T4 abundance, we fed C2GnT3-deficient mice and wild-type littermates chow supplemented with 0.025% porcine thyroid powder (34). Wild-type and C2GnT3-deficient mice fed thyroid-powder supplemented chow achieved similar circulating T4 levels (Figure 6c). When these mice were retested in the social dominance assay, no difference between C2GnT3-deficient and wild-type mice was observed (Figure 6d). This finding indicates that the altered behavior observed in C2GnT3-deficient mice is likely due to reduced T4 levels in circulation.

The thyroid is stimulated to release T4 in response to secretion of Thyroid Stimulating Hormone (TSH) from the pituitary. Thus we investigated the abundance of TSH in circulation in C2GnT3-deficient mice. No difference was observed in circulating TSH abundance (Figure 6e). Reduced levels of circulating T4, in the presence of normal levels of TSH, suggests secondary hypothyroidism because thyroid hormone regulation involves a negative feedback loop in which T4 feeds back to the pituitary to reduce TSH secretion (11, 16). Secondary hypothyroidism can be tested by stimulation with thyrotropin-releasing hormone (TRH), the hormone secreted from

the hypothalamus that stimulates the pituitary to release TSH (41, 67). No differences were present in the levels of T4 secreted in response to TRH stimulation among wild-type and C2GnT3-deficient mice (Figure 6f). This suggests that the slight reduction in T4 levels may not be sufficient to increase TSH levels via the negative feedback loop.

The mild hypothyroidism in C2GnT3-deficient mice may not be a result of secondary hypothyroidism despite normal levels of TSH. To determine if T4 levels are reduced due to decreased half-life in circulation, we compared the *in vivo* half-life of T4 in wild-type and C2GnT3-deficient mice. No difference in T4 half-life in wild-type and C2GnT3-deficient mice was detected (Figure 6g).

Mice deficient for all three C2GnTs are viable

The extent to which the three known glycosyltransferases with C2GnT activity can biologically compensate for each other is unknown, thus we chose to generate mice deficient for multiple C2GnTs. As these three *Gcnt* genes reside on different chromosomes, we accomplished this by crossing the single deficient states to each other. All three possible C2GnT doubly deficient combinations (T1/T2, T1/T3, T2/T3) were generated, and these animals were born without overt abnormalities and appeared normal. From these parental sources, offspring should theoretically include triple-null littermates (T1/T2/T3). Remarkably, mice deficient in all three C2GnTs were born viable and appeared to develop normally to adults. In addition, both male and female T1/T2/T3 mice were fertile (data not shown).

C2GnT and C4GnT activity in C2GnT deficient mice

C2GnT2 and C2GnT4 enzymatic activity levels were determined among tissue lysates from animals bearing single and multiple C2GnT deficiencies. C2GnT2-deficient colon and mesenteric lymph node samples contained significantly reduced C2GnT activity compared to the level of activity in wild-type lysates (Figure 7a). Furthermore, no significant C4GnT activity was detected in any tissue tested from C2GnT2-deficient mice, implying that C4GnT activity is produced exclusively by C2GnT2 (50, 69). In contrast, no significant decrease in C2GnT activity was measured among various tissues analyzed from C2GnT3-deficient mice, despite the fact that the entire coding region of C2GnT3 was similarly deleted (Figure 7b). Nevertheless, very little C2GnT activity was detected in tissues from mice deficient for all three C2GnTs (Figure 7c).

O-glycans structures in C2GnT deficiency

O-glycan structures from C2GnT2 and C2GnT3 singly deficient mouse tissues were compared to wild-type samples using mass spectrometric glycomic methodologies (25). The O-glycan structural changes reported herein have been selected among a larger number of alterations with a focus on the major defects observed. The full O-glycomes of each tissue remain to be established but will be reported elsewhere. Decreases in Core 2 O-glycan structures, along with increases in various Core 1 O-glycan structures, were clearly detected in C2GnT2-deficient stomach, colon, and small intestine samples (Table I). In C2GnT2-deficient stomach and colon tissues, the increased abundance of Core 1 structures included elongated Core 1 branches, several of which bore polylactosamine. In contrast, in the small intestine non-elongated, sialylated Core 1 O-glycan structures were increased. Furthermore, stomach and

colon tissues from C2GnT2-deficient mice exhibited a decrease in I-branching. Surprisingly, elongated O-mannose structures were detected in the stomach of C2GnT2-deficient mice but not wild-type counterparts. O-glycans structures from C2GnT2-deficient kidney samples were unaltered as compared to wild-type kidney structures, consistent with the relative expression of murine C2GnT2.

C2GnT3-deficient tissues contained O-glycan structural changes in the small intestine, stomach and thyroid/trachea samples with decreases in the relative abundance of some Core 2 O-glycan structures relative to Core 1 O-glycan structures in these tissues. No substantial changes in O-glycan structures were noted in the thymus, colon, kidney or liver from C2GnT3-deficient mice (Table I and data not shown). These findings revealed that even in tissues with high relative expression of C2GnT3, loss of this glycosyltransferase did not lead to marked changes in O-glycan structures.

Tissues from T1/T2/T3 mice deficient in all three known C2GnTs lacked all detectable Core 2 O-glycan structures among all tissues surveyed including the colon, small intestine, stomach, and kidney (Table I). These results indicate that no other glycosyltransferases appear capable of synthesizing Core 2 O-glycans *in vivo*. Furthermore, small intestine, stomach, and colon samples from T1/T2/T3 mice had a further increase in elongated Core 1 O-glycans compared to tissues lacking a single C2GnT. Surprisingly, no O-glycan structures containing I-branches were detected in stomach and colon samples from T1/T2/T3 mice. There was also an unexpected increase in elongated O-mannose structures in the stomach of T1/T2/T3 mice, even in comparison with C2GnT2-deficient stomach samples.

Discussion

The presence of three conserved genes encoding glycosyltransferases that can initiate the biosynthesis of Core 2 O-glycans suggests that each C2GnT may provide significant compensation for each other as afforded by this close overlap in enzymatic activity. However, the different expression profiles of each C2GnT among tissues and cell types, as well as some inherent enzymatic differences, also suggests unique biological roles may exist involving each C2GnT glycosyltransferase. By generating mice singly and multiply deficient in C2GnT activities, we have developed models to study the structure and function of O-glycosylation as controlled by C2GnT activity. Core 2 and perhaps Core 4 O-glycans produced by C2GnT2 operate in establishing the epithelial mucosal barrier and reduce disease signs following chemical induction of colitis. Alterations in humoral and mucosal immune system homeostasis were present and may be related to these findings. In contrast, C2GnT3 does not provide a role in formation or maintenance of the mucosal barrier, but instead its deficiency alters behavorial phenotypes linked with reduced T4 Thyroxine abundance in circulation. Neither C2GnT2 nor C2GnT3 appear to function in the biosynthesis of selectin ligands, unlike previous findings in mice lacking C2GnT1 (14). Each C2GnT glycosyltransferase has different biological roles as evidenced in these physiological systems *in vivo*. Both expected and unexpected changes occurred in the repertoire of O-glycans detected among multiple tissues from animals deficient in C2GnT activity. These structural alterations of the glycome will aid in identifying further the mechanistic features of O-glycan biosynthesis and the etiology of these phenotypes.

Distinct and potential overlapping functions of C2GnTs

Neutrophila in the absence of a measured defect in selectin ligand expression by cytometry in C2GnT3-deficient mice is reminiscent of mice deficient for α(1,3)fucosyltransferase-IV (FucT-IV). In contrast, no hematological or selectin ligand biosynthetic defect was observed in C2GnT2 deficiency. Mice deficient for FucT-IV also exhibited a slight increase (20%) in neutrophils in circulation without measurable decreases in binding of selectin chimeras to neutrophils (23). Nevertheless, FucT-IV was shown to contribute to selectin ligand function *in vivo,* as FucT-IV-deficiency increased selectin-dependent leukocyte rolling velocity in microvessels (65). It remains possible that C2GnT3 contributes to selectin ligand formation detectable by additional studies and approaches. Alternatively, C2GnT3 may modulate neutrophil abundance in circulation by altering myelopoiesis. Several cell adhesion molecules, including selectins and sialomucins, have been found influence hematopoiesis and altered glycosylation has been shown to increase neutrophil production (23, 53, 63). This may reflect altered binding between lectins and glycoproteins in the context of stem cell turnover and differentiation. Nevertheless, the degree of increase observed among circulating neutrophils *per se* in C2GnT3-deficient mice is unlikely to significantly alter physiology.

Decreased mucosal barrier function is associated with Inflammatory Bowel Diseases (IBDs) (33, 55), including colitis. It is possible that the increased mucosal permeability and disease signs that occur with DSS treatment are related in C2GnT2-deficient mice. Moreover, the single C3GnT glycosyltransferase that generates Core 3 O-glycans is also essential for mucosal barrier function and similarly decreases susceptibility to DSS-induced colitis (2). In C3GnT-deficient mice, those findings were attributed to reduced abundance of Muc2, a mucin known to be necessary for protection from colitis (2, 60). In contrast, C2GnT2 deficient mice

did not appear to have decreased expression of Muc2. Susceptibility to IBDs is associated with factors other than altered mucin levels, including changes in commensal and pathogenic organisms as well as altered immune system homeostasis (43, 66). In C2GnT2-deficient mice, the impaired humoral immune homeostasis exhibited by reduced serum IgG1, IgG2a, IgG2b, and mucosal IgA levels may indicate or contribute somehow to increased susceptibility to experimental colitis. Furthermore, as high relative expression of C2GnT2 is prominent among tissues with high epithelial cell content, it is possible that the decrease in some immunoglobulin subtypes is due to a defect of the mucosal immune system. Perhaps the C2GnT2 and C3GnT glycosyltransferases collaborate to enforce the mucosal epithelial barrier.

Several mechanisms may explain the reduced T4 Thyroxine abundance in C2GnT3-deficient mice. Alterations in the T4 negative feedback loop could lead to decreased T4 abundance in the presence of normal TSH levels. Alternatively, it remains possible that decreased T4 half-life or T4 secretion in response to TSH stimulation in C2GnT3 deficiency occurs at levels below experimental detection. Additional studies that include analyses of T4-carrier proteins may further resolve this. From our findings it remains possible that overly aggressive behavior linked to decreased T4 abundance may be among the first symptoms to develop in some cases of hypothyroidism.

While mice singly deficient for C2GnT1, C2GnT2 or C2GnT3 exhibited distinct phenotypes, the presence of novel phenotypes in mice deficient for multiple C2GnTs, but not present in any of the singly deficient models, would reveal collaboration and compensation among these glycosyltransferases in physiologic processes. Preliminary data indicates that T1/T2/T3 mice are unqiue among the other lesser deficiency states with elevated levels of the liver enzyme alanine transaminase (ALT), implying changes in liver function apparent only in

the absence of all three C2GnTs (unpublished observation). Defining the biological mechanisms of the phenotypes evoked by the loss of C2GnT activity will require additional resolution that is afforded by linking glycan structures to normal and pathologic contexts.

Structural basis of O-glycan biosynthesis determined by C2GnT1, C2GnT2 and C2GnT3

The absence of any single C2GnT glycosyltransferase results in a reduction of Core 2 O-glycan structures in one or more tissues *in vivo.* By comparison, the decrease in Core 2 O-glycan structures in C2GnT3-deficient tissue samples was modest and C2GnT activity was not mearsurable decreased in these tissues. This suggests that C2GnT3 may have a relatively minor contribution to Core 2 O-glycan biosynthesis in these tissue types *in vivo*. Core 2 O-glycan structures were totally absent from tissues lacking all three C2GnTs. Interestingly, tissue lysates from these triply-deficient animals harbored a small amount of C2GnT enzymatic activity. This suggests the possibility that another unidentified glycosyltransferase may have a low level of C2GnT activity when assayed *in vitro.* Nevertheless, the absence of Core 2 O-glycan structures in T1/T2/T3 mice indicates that no additional glycosyltransferases exist that can generate Core 2 O-glycans *in vivo* as detected by our analyses.

C2GnT deficiency further altered the repertoire and abundance of O-glycan structures not directly generated by C2GnTs and produced by different biosynthetic pathways. The large decrease in the abundance of I-branching on O-glycan structures from stomach and colon tissues of mice lacking C2GnT2 suggests that in some tissues C2GnT2, and not IGnT, is the dominant I-branching glycosyltransferase in protein O-glycosylation. The further degree of loss of I-branching in stomach and colon samples from mice lacking all three C2GnTs implies that either C2GnT1 or C2GnT3 may also have I-branching activity *in vivo*. In this regard, C2GnT3 has

been characterized with a low level of I-branching activity *in vitro* (51). The repertoire of Core 1 O-glycans and O-mannosylated glycans were also altered among various tissues. The increase of Core 1 O-glycan structures and their elongation in the absence of one or more C2GnTs was linked with the formation of polylactosamines that may alter lectin-dependent binding and physiology. This elaboration of Core 1 O-glycans is not likely due to reduced competition for acceptor substrates in the Golgi apparatus, as the formation of the Core 2 O-glycan branch does not decrease the efficiency of Core 1 extension enzyme-β1,3-*N*-acetylglucosaminyltransferase (C1GnT) (68). Alternate explanations include possible the possible elevation of C1GnT activity or perhaps an increase in the availability of the common UDP-GlcNAc donor substrate, which is also used in the process protein O-mannosylation (70, 72). Core 4 O-glycan structures if present exist below the level of detection in wild-type and C2GnT deficient tissues, thus it is not currently known whether the loss of C4GnT activity in C2GnT2 deficiency correlates with a reduction or absence of Core 4 O-glycans *in vivo*.

Core 2 O-glycans have been associated with interactions among commensal and pathogenic bacteria, and their hosts. Loss of C2GnT2 may alter the ability of commensal or pathogenic bacteria to colonize the host. Recently it has been shown that *Helicobacter pylori* and *Clostridium perfringens* express proteins that bind to Core 2 O-glycans (5, 27). Preliminary data also suggests that C2GnT3 may be required for T-cell responses to an intestinal challenge (H. Ziltener, personal communication). These findings may relate to the phenotypes we have thus far reported in C2GnT deficiency states and suggest that challenging these animals with additional stimuli may further reveal novel biological roles of Core 2 O-glycans. Nevertheless, the relatively mild impact of Core 2 O-glycan deficiency *in vivo* may reflect partial to full compensation provided by the resulting induction of extended Core 1 and o-mannosylated O-

glycan structures, as was similarly established in the formation of selectin ligands on estended Core 1 O-glycans in C2GnT-1 deficiency (68). C2GnT deficiency modeled among intact mice has contributed substantially to understanding the biosynthesis and functions of protein O-glycosylation in vivo. Each of the three glycosyltransferases with C2GnT activity has a distinct function, and thus begins to explain why three separate genes encoding C2GnT enzymes have been selected and conserved in mammalian evolution.

Acknowledgements

We thank David Ditto for technical expertise with hematological assays and Margo Streets and Trang Tran for technical expertise with behavior assays. Jeffery Long assisted with statistical analysis of behavioral data.

This work was funded in part by a Mizutani Foundation for Glycoscience award (J.D.M.), Veterans Affairs Merit Review Grant (S.B.H.), the University of California San Diego Digestive Disease Research Development Center (S.B.H) and National Institute of Health grants HL057345 (J.D.M.), HL78784 (J.D.M.), GMG2116 (J.D.M.), CA33000 (MF) and P01CA71932 (M.F., J.D.M.). J.D.M. is supported by the Howard Hughes Medical Institute. This work was also funded in part by the Biotechnology and Biological Sciences Research Council, BBF0083091 (A.D.) and Public Health Service grant DK080506 (S.B.H.). M.N.I. is supported by University Science Malaysia, Ministry of Higher Education. The authors declare that they have no competing financial interests.

References

1. Altschuler, Y., Kinlough, C.L., Poland, P.A., Bruns, J.B., Apodaca, G., Weisz, O.A. and Hughey, R.P. 2000. Clathrin-mediated endocytosis of MUC1 is modulated by its glycosylation state. Mol. Biol. Cell *11*: 819-831.

2. An, G., Wei, B., Xia, B., McDaniel, J.M., Ju, T., Cummings, R.D., Braun, J. and Xia, L. 2007. Increased susceptibility to colitis and colorectal tumors in mice lacking core 3-derived O-glycans. J. Exp. Med. *204*: 1417-1429.

3. Arkan, M.C., Hevener, A.L., Greten, F.R., Maeda, S., Li, Z.W., Long, J.M., Wynshaw-Boris, A., Poli, G., Olefsky, J. and Karin, M. 2005. IKK0beta links inflammation to obesity-induced insulin resistance. Nat. Med. *11*:191-198.

4. Aronson, L. 1998. Animal behavior case of the month. Aggression directed toward other horses. J. Am. Vet. Med. Assoc. *213*: 358-359.

5. Ashida, H., Maki, R., Ozawa, H., Tani, Y., Kiyohara, M., Fujita, M., Imamura, A., Ishida, H., Kiso, M. and Yamamoto, K. 2008. Characterization of two different endo-α-*N*-acetylgalactosaminidases from probiotic and pathogenic enterobacteria, *Bifidobacterium longum* and *Clostridium perfringens.* Glycobiol. *18*: 727-734.

6. Baum, L.G. 2002. Developing a Taste for Sweets. Immunity *16*; 5-8.

7. Bierhuizen, M.F. and Fukuda, M. 1992. Expression cloning of a cDNA encoding UDP-GlcNAc:Gal beta 1-3-GalNAc-R (GlcNAc to GalNAc) beta 1-6GlcNAc transferase by gene transfer into CHO cells expressing polyoma large tumor antigen. Proc. Natl. Acad. Sci. *89*: 9326-9330.

8. Carlow, D.A., Ardman, B., and Ziltener, H.J. 1999. A novel CD8 T cell-restricted CD45RB epitope shated by CD43 is differentially affected by glycosylation. J. Immunol. *163*: 1441-1448.

9. Cho, J.H. 2008. The genetics and immunopathogenesis of inflammatory bowel disease. Nat. Rev. Immunol. *8*: 458-466.

10. Crawley, J.N. 2007. What's wrong with my mouse? Behavioral phenotyping of transgenic and knockout mice. 1st ed. New York, New York. Wiley Interscience.

11. Dahl, G.E., Evans, N.P., Thrun, L.A. and Karsch, F.J. 1994. A central negative feedback action of thyroid hormones on thyrotropin-releasing hormone secretion. Endocrinol. *135*: 2392-2397.

12. Dodman, N.H., Mertens, P.A. and Aronson, L.P. 1995. Animal behavior case of the month. Dogs were evaluated because of aggression. J. Am. Vet. Med. Assoc. *207*:1168-1171.

13. deVos, T. and Dick, T.A. 1991. A rapid method to determine the isotype and specificity of coproantibodies in mice infected with Trichinella or fed cholera toxin. J. Immunol. Methods *141*: 285-288.

14. Ellies, L.G., Tsuboi, S., Petryniak, B., Lowe, J.B., Fukuda, M. and Marth, J.D. 1998. Core 2 oligosaccharide biosynthesis distinguishes between selectin ligands essential for leukocyte homing and inflammation. Immunity *9*:881-890.

15. Fatjo, J., Amat, M. and Manteca, X. 2003. Animal behavior case of the month. Aggression in dogs. J. Am. Vet. Med. Assoc. *223*: 623-626.

16. Fliers, E., Unmehopa, U.A. and Alkemade, A. 2006. Functional neuroanatomy of thyroid hormone feedback in the human hypothalamus and pituitary gland. Mol. Cell Endocrinol. *251*: 1-8.

17. Furuta, G.T., Turner, J.R., Taylor, C.T., Hershberg, R.M., Comerford, K., Narravula, S., Podolsky, D.K. and Colgan, S.P. 2001. Hypoxia-inducible Factor 1-dependent Induction of Intestinal Trefoil Factor Protests Barrier Function during Hypoxia. J.Exp. Med. *193*:1027-1034.

18. Gauguet, J.M., Rosen, S.D., Marth, J.D. and von Andrian, U.H. 2004. Core 2 Branching β1,6-N-acetylglucosaminyltransferase and high endothelial cell N-acetylglucosamine-6-sulfotransferase exert differential control over B- and T-lymphocyte homing to peripheral lymph nodes. Blood *104*:4104-4112.

19. Grewal, P.K., Uchiyama, S., Ditto, D., Varki, N., Le, D.T., Nizet, V. and Marth, J.D. 2008. The Ashwell Receptor mitigates the lethal coagulopathy of sepsis. Nat, Med. *14*: 648-655.

20. Hassan, H., Reis, C.A., Bennett, E.P., Mirgorodskaya, E., Roepstorff, P., Hollingsworth, M.A., Burchell, J., Taylor-Papadimitriou, J and Clausen, H. 2000. The lectin domain of UDP-N-acetyl-D-galactosamine: polypeptide N-acetylgalactosaminyltransferase-T4 directs its glycopeptide specificities. J. Biol. Chem. *275*: 38197-38205.

21. Hiraoka, N., Kawashima, H., Petryniak, B., Nakayama, J., Mitoma, J., Marth, J.D., Lowe, J.B. and Fukuda, M. 2004. Core 2 Branching β1,6-N-Acetylglucosaminyltransferase and High Endothelial Venule-restricted Sulfotransferase collaboratively control lymphocyte homing. J. Biol. Chem. *279*:3058-3067.

22. Ho, S.B., Dvorak, L.A., Moor, R.E., Jacobson, A.C., Frey, M.R., Corredor, J., Polk, D.B. and Shekels, L.L. 2006. Cysteine-rich domains of Muc3 intestinal mucin promote cell migration, inhibit apoptosis, and accelerate wound healing. Gastroenterology *131*:1501-1517.

23. Homeister, J.W., Thall, A.D., Petryniak, B., Maly, P., Rogers, C.E., Smith, P.L., Kelly, R.J., Gersten, K.M., Askari, S.W., Cheng, G., Smithson, G., Marks, R.M., Misra, A.K., Hindsgaul, O., von Andrian, U.H. and Lowe, J.B. 2001. The alpha(1,3)fucosyltransferases FucT-IV and FucT-VII exert collaborative control over selectin-dependent leukocyte recruitment and lymphocyte homing. Immunity *15*:115-126.

24. Iwai, T., Inaba, N., Naundorf, A., Zhang, Y., Gotoh, M., Iwasaki, H., Kudo, T., Togayachi, A., Ishizuka, Y., Nakanishi, H. and Narimatsu, H. 2002. Molecular cloning and characterization of a novel UDP-GlcNAc:GalNAc-peptide beta1,3-N-acetylglucosaminyltransferase (beta 3Gn-T6), an enzyme synthesizing the core 3 structure of O-glycans. J. Biol. Chem. *277*: 12802-12809.

25. Jang-Lee, J., North, S.J., Sutton-Smith, M., Goldberg, D., Panico, M., Morris, H., Haslam, S. and Dell, A. 2006. Glycomic profiling of cells and tissues by mass spectrometry:fingerprinting and sequencing methodologies. Methods Enzymol. *415*: 59-86.

26. Ju, T., Brewer, K., D'Souza, A., Cummings, R.D. and Canfield, W.M. 2002. Cloning and expression of human core 1 beta1,3-galactosyltransferase. J. Biol. Chem. *277*: 178-186.

27. Kawakubo, M., Ito, Y., Okimura, Y., Kobayashi, M., Sakura, K., Kasama, S., Fukuda, M.N., Fukuda, M., Katsuyama, T. and Nakayama, J. 2004. Natural antibiotic function of a human gastric mucin against *Helicobacter pylori* infection. Science *305*:1003-1006.

28. Long, J.M., LaPorte, P., Merscher, S., Funke, B., Saint-Jore, B., Puech, A., Kucherlapati, R., Morrow, B.E., Skoultchi, A.I. and Wynshaw-Boris, A. 2006. Behavior of mice with mutations in the conserved region deleted in velocardiofacial/DiGeorge syndrome. Neurogenetics *7*:247-257.

29. Long, J.M., LaPorte, P., Paylor, R. and Wynshaw-Boris, A. 2004. Expanded characterization of the social interaction abnormalities in mice lacking *Dvl1*. Genes Brain Behav. *3*: 51-62.

30. Lowe, J.B. 2001. Glycosylation, Immunity, and Autoimmunity. Cell *104*; 809-812.

31. Lowe, J.B. and Marth, J.D. 2003. A genetic approach to Mammalian glycan function. Annu. Rev. Biochem. *72*:643-691.

32. Magnet, A.D. and Fukuda, M. 1997. Expression of the large I antigen forming β-1,6-*N*-acetylglucosaminyltransferase in various tissues of adult mice. Glycobiology *7*: 285-295.

33. Mankertz, J. and Schulzke, J.D. 2007. Altered permeability in inflammatory bowel disease: pathophysiology and clinical implications. Curr. Opin. Gasteroenterol. *23*: 379-383.

34. Marians, R.C., Ng, L., Blair, H.C., Unger, P., Graves, P.N. and Davies, T.F. 2002. Defining thyrotropin-dependent and –independent steps of thyroid hormone synthesis by using thyrotropin receptor-null mice. Proc. Natl. Acad. Sci. *99*: 15776-15781.

35. Marth., J.D and Grewal, P.K. 2008. Mammalian glycosylation in immunity. Nat. Rev. Immunol. *8*: 874-887.

36. Merzaban, J.S., Zuccolo, J., Corbel, S.Y., Williams, M.J. and Ziltener, H.J. 2005. An alternate Core 2β1,6-*N*-Acetylglucosaminyltransferase selectively contributes to P-selectin ligand formation in activated CD8 T cells. J. Immunol. *174*: 4051-4059.

37. Murthy, A.K., Dubose, C.N., Banas, J.A., Coalson, J.J. and Arulanandam, B.P. 2006. Contribution of polymeric immunoglobulin receptor to regulation of intestinal inflammation in dextran sulfate sodium-induced colitis. Gastroenterol. *26*: 1372-1380.

38. Murthy, S.N., Cooper, H.S., Shim, H., Shah, R.S., Ibrahim, S.A. and Sedergran, D.J. 1993. Treatment of dextran sulfate sodium-induced murine colitis by intracolonic cyclosporine. Dig. Dis. Sci. *38*: 1722-1734.

39. Nagy, A., Rossant, J., Nagy, R., Abramow-Newerly, W. and Roder, J.C. 1993. Derivation of completely cell culture-derived mice from early-passage embryonic stem cells. Proc. Natl. Acad. Sci. USA. *90*: 8424-8428.

40. Okayasu, I., Hatakeyama, S., Yamada, M., Ohkusa, T., Inagaki, Y. and Nakaya, R. 1990. A novel method in the induction of reliable experimental acute and chronic ulcerative colitis in mice. Gastroenterol. *98*: 694-702.

41. Oliverira, K.J., Ortiga-Carvalho, T.M., Cabanelas, A., Veiga, M.A.L.C., Aoki, K., Ohki-Hamazaki, H., Wada, K., Wada, E. and Pazos-Moura, C.C. 2006. Disruption of neuromedin B receptor gene results in dysregulation of the pituitary-thyroid axis. J. Mol. Endocrinol. *36*: 73-80.

42. Perez-Vilar, J. and Hill, R.L. 1999. The structure and assembly of secreted mucins. J. Biol. Chem. *274:* 31751-31754.

43. Peterson, D.A., Frank, D.N., Pace, N.R and Gordon, J.I. 2008. Metagenomic Approaches for defining the pathogenesis of inflammatory bowel disease. Cell Host & Microbe *3*:417-427.

44. Raman, J., Fritz, T.A., Gerken, T.A., Jamison, O., Live, D., Liu, M. and Tabak, L.A. 2008. The catalytic and lectin domains of UDP-GalNAc:Polypeptide α-*N*-acetylgalactosaminyltransferasae function in concert to direct glycosylation site selection. J. Biol. Chem. *283:* 22942-22951.

45. Rosen, S.D. 2004. Ligands for L-selectin: homing, inflammation, and beyond. Annu. Rev. Immunol. *22*: 129-156.

46. Rossi, F.M.V., Corbel, S.Y., Merzaban, J.S., Carlow, D.A., Gossens, K., Duenas, J., So, L., Yi, L. and Ziltener, H.J. 2005. Recruitment of adult thymic progenitors is regulated by P-selectin and its ligand PSGL-1. Nat. Immunol. *6*:626-634.

47. Satsangi, J., Parkes, M., Louis, E., Hashimoto, L., Kato, N., Welsh, K., Terwilliger, J.D., Lathrop, G.M., Bell, J.I. and Jewell, D.P. 1996. Two stage genome-wide search in inflammatory bowel disease provides evidence for susceptibility loci on chromosomes 3, 7 and 12. Nature Genet. *14*: 199-202.

48. Schachter, H. 2000. The joys of HexNAc. The synthesis and function of N- and O-glycan branches. Glycoconj. J. *17*: 465-483.

49. Schachter, H. and Brockhausen, I. 1989. The biosynthesis of branched O-glycans. Symp. Soc. Exp. Biol. *43*: 1-26.

50. Schwientek, T., Nomoto, M., Levery, S.B., Merkx, G., van Kessel, A.G., Bennett, E.P., Hollingsworth, M.A. and Clausen, H. 1999. Control of O-glycan branch formation. Molecular cloning of human cDNA encoding a novel beta1,6-N-acetylglucosaminyltransferase forming core 2 and core 4. J. Biol. Chem. *274*: 4504-4512.

51. Schwientek, T., Yeh, J.C., Levery, S.B., Keck, B., Merkx, G., van Kessel, A.G., Fukuda, M. and Clausen, H. 2000. Control of O-glycan branch formation: Molecular cloning and characterization of a novel thymus-associated Core 2 β1,6-N-acteylglucosaminyltransferase. J. Biol. Chem. *275*:11106-11113.

52. Shafi, R., Iyer, S.P., Ellies, L.G., O'Donnell, N., Marek, K.W., Chui, D., Hart, G.W. and Marth, J.D. 2000. The O-GlcNAc transferase gene resides on the X chromosome and is essential for embryonic stem cell viability and mouse ontogeny. Proc. Natl. Acad. Sci. USA. *97:* 5735-5739.

53. Simmons, P.J., Levesque, J., Haylock, D.N. 2001. Mucin-like molecules as modulators of the survival and proliferation of primitive hematopoietic cells. Ann. N. Y. Acad. Sci. *938*: 196-207.

54. Stanley, P. 2007. Regulation of Notch signaling by glycosylation. Curr. Opin. Struct. Biol. *17*:530-535.

55. Stein, J., Ries, J. and Barrett, K.B. 1998. Disruption of intestinal barrier function associated with experimental colitis: possible role of mast cells. Am. J. Physiol. *274*: G203- G209.

56. Sutton-Smith, M., Morris, H.R. and Dell, A. 2000. A rapid mass spectrometric strategy suitable for the investigation of glycan alterations in knockout mice. Tetrahedron: Asymmetry. *11:* 363-369.

57.Tarp, M.A. and Clausen, H. 2008. Mucin-type *O*-glycosylation and its potential use in drug and vaccine development. Biochim. Biophys. Acta *1780*: 546-563.

58. Ten Hagen, K.G., Fritz, T.A. and Tabak, L.A. 2003. All in the family: the UDP-GalNAc:polypeptide N-acetylgalactosaminyltransferases. Glycobiol. *13*; 1R-16R.

59. Tenno, M., Ohtsubo, K., Hagen, F.K., Ditto, D., Zarbock, A., Schaerli, P., von Andrian, U.H., Ley, K., Le, D., Tabak, L.A. and Marth, J.D. 2007. Initiation of protein O glycosylation by polypeptide GalNAcT-1 in vascular biology and humoral immunity. Mol. Cell Biol. *27*: 8783-8796.

60. van der Sluis, M., de Koning, B.A.E., de Bruijn, A.C.J.M., Velcich, A., Meijerink, J.P.P., van Goudoever, J.B., Buller, H.A. and Einerhand, A.W.C. 2006. Muc2-deficient mice spontaneously develop colitis, indicating that Muc2 is critical for colonic protection. Gastroenterol. *131*:117-129.

61. Varki, A. 2006. Nothing in Glycobiology makes sense, except in the light of evolution. Cell *126*; 841-845.

62. Venero, C., Guadano-Ferraz, A., Herrero, A.I., Nordstrom, K., Manzano, J., de Escobar, G.M., Bernal, J. and Vennstrom, B. 2005. Anxiety, memory impairment, and locomotor dysfunction caused by a mutant thyroid hormone receptor α1 can be ameliorated by T3 treatment. Genes & Development *19*:2152-2163.

63. Verfaillie, C.M. 1998. Adhesion receptors as regulators of the hematopoietic process. Blood *92*: 2609-2612.

64. Wang, H., Tang, R., Zhang, W., Amirikian, K., Geng, Z., Geng, J., Hebbel, R.P., Xia, L., Marth, J.D., Fukuda, M., Katoh, S. and Huo, Y. 2008. Core2 1-6-N-Glucosaminyltransferase-I is crucial for the formation of atherosclerotic lesions in apolipoprotein E-deficient mice. Arterioscler. Thromb. Vasc. Biol. *In press.*

65. Weninger, W., Ulfman, L.H., Cheng, G., Souchkova, N., Quackenbush, E.J., Lowe, J.B. and von Andrian, U.H. 2000. Specialized contributions by α(1,3)-Fucosyltransferase-IV and FucT-VII during leukocyte rolling in dermal microvessels. Immunity *12*: 665-676.

66. Xavier, R.J. and Podolsky, D.K. 2007. Unraveling the pathogenesis of inflammatory bowel disease. Nature *448*: 427-434.

67. Yamada, M., Saga, Y., Shibusawa, N., Hirato, J., Murakami, M., Iwasaki, T., Hashimoto, K., Satoh, T., Wakabayashi, K., Taketo, M.M. and Mori, M. 1997. Tertiary hypothyroidism and hyperglycemia in mice with targeted disruption of the thyrotropin-releasing hormone gene. Proc. Natl. Acad. Sci. *94*: 10862-10867.

68. Yeh, J.C., Hiraoka, N., Petryniak, B., Nakayama, J., Ellies, L.G., Rabuka, D., Hindsgaul, O., Marth, J.D., Lowe, J.B. and Fukuda, M. 2001. Novel sulfated lymphocyte homing receptors and their control by a Core1 extension beta 1,3,-N-acetylglucosaminyltransferase. Cell *105*: 957-969.

69. Yeh, J.C., Ong, E. and Fukuda, M. 1999. Molecular cloning and expression of a novel β-1,6-N-Acetylglucosaminyltransferase that forms Core 2, Core 4, and I branches. J. Biol. Chem. *274*:3215-3221.

70. Yoshida, A., Kobayashi, K., Manya, H., Taniguchi, K., Kano, H., Mizuno, M., Inazu, T., Mitsuhashi, H., Takahashi, S., Takeuchi, M., Herrmann, R., Straub, V., Talim, B., Voit, T., Topaloglu, H., Toda, T. and Endo, T. 2001. Muscular dystrophy and neuronal migration disorder caused by mutations in a glycosyltransferase, POMGnT1. Dev. Cell *1*: 717-724.

71. Zachara, N.E. and Hart, G.W. 2006. Cell signaling, the essential role of O-GlcNAc! Biochem. Biophys. Acta. *1761*:599-617.

72. Zhang, W., Betel, D. and Schachter, H. 2002. Cloning and expression of a novel UDP-GlcNAc:a-3-D-mannoside b1,2-*N*-acetylglucosaminyltransferase I. Biochem. J. *361*: 153-162.

Figure 1

Activity and expression of C2GnTs

(a-c) Monosaccharides are depicted as geometric shapes with GalNAc as a yellow square, galactose as a yellow circle, and GlcNAc as a blue square. In addition, the vertical arrows indicate that each branch can be further elaborated by additional saccharide linkages. (a) Biantennary Core 2 O-glycans are generated when any of the three C2GnTs acts on the Core 1 O-glycan disaccharide. (b) C2GnT2 can generate Core 4 O-glycans from Core 3 O-glycans by adding a GlcNAc to the initiating GalNAc. (c) C2GnT2, in addition to IGnT, also has the ability to generate branched polylactosamine repeats from linear polylactosamine repeats. The figure depicts distal I-branching as the GlcNAc is transferred to the predistal galactose, the preferential I-branching activity of C2GnT2. However, IGnT preferentially has central I-branching activity that adds GlcNAc on the internal galactose in Galβ1→4GlcNAcβ1→3Gal-R (69). (d) RNA expression of murine *Gcnt3* (left panel) and *Gcnt4* (right panel), which code for C2GnT2 and C2GnT3, respectively, as determine by qPCR. Data is graphed relative to testes expression. All values are means ± S.E.M.

Figure 2

Generation of mice singly deficient for C2GnT2 or C2GnT3

(a*) Gcnt3* genomic clone from 129/SvJ mouse strain was used to generate a targeting construct using the pflox vector as indicated. B: Bgl II, Ba: Bam HI, E: Eco RI, S: Spe I, X: Xba I, Xh: Xho I. (b) Southern blotting of genomic DNA confirms the *Gcnt3* allele structure present in ES cells using the genomic probe (top). Southern blotting with a loxP probe detects the location and number of loxP sites (bottom). (c) The targeting of the single coding exon of *Gcnt4* using the

pflox vector in depicted. A: Age I, B: Bam HI, E: Eco RV, S: Sac I, Sa: Sal I, St: Stu I, X: Xho I. (d) Southern blots of genomic DNA with the genomic probe (top) or loxP probe (bottom) indicate the structure of *Gcnt4* alleles present.

Figure 3

Selectin ligand expression on neutrophils and T-cells from C2GnT-deficient mice

(a) Hematological levels in mice single deficient for C2GnT2 or C2GnT3 relative to wild-type levels are graphed. (b and c) Histograms depict the expression of ligands for P- and E-selectins on neutrophils from mice singly deficient for (b) C2GnT3 or (c) C2GnT2. Addition of EDTA controls for binding of C-type lectins. (d) Number of thymocytes of each cell type in wild-type and C2GnT3-deficient mice is graphed (DN: $CD4^-$, $CD8^-$ cells; DP: $CD4^+$, $CD8^+$ cells; SP: $CD4^+$ or $CD8^+$ cells). (e) Expression of the 1B11 antigen on thymocyte sub-populations is shown. (f) Histograms indicate the level of expression of activation markers and selectin ligands on activated wild-type and C2GnT3-deficient T-cells. All values are means ± S.E.M. (*$p<0.05$)

Figure 4

Barrier function and colitis in C2GnT2-deficient mice

(a) The amount of dextran-FITC in sera four hours after administration by gavage is graphed. Data shown is from a minimum of 6 mice per a genotype. (b) Graph shows the average percent weight change as compared to t=0 of wild-type (closed squares) and C2GnT2-deficient (open squares) mice during and following treatment with 5% DSS until onset of mortality. The horizontal line represents the time of the DSS treatment. DSS was given to 6 mice of each genotype. (c) DAI of wild-type and C2GnT2-deficient mice treated with 5% DSS is graphed.

(d) The length of grade III damage (total ulceration with loss of glands and surface epithelium) in colon sections from of DSS-treated wild-type and C2GnT2-deficient mice is shown. (e) The average crypt damage score is graphed. (f) Representative H&E stained colon sections from DSS-treated wild-type mice (illustrating grade II and grade I crypt damage) and C2GnT2-deficient mice (illustrating grade III crypt damage or total ulceration). (g) Relative mucosal Muc2 levels from untreated wild-type and C2GnT2-deficient mice is graphed. All values are means ± S.E.M. S.E.M. is represented by capped and uncapped vertical lines. ($p<0.05$)

Figure 5

Circulating and mucosal immunoglobulins in wild-type and C2GnT2-deficient mice.

(a) Circulating levels of immunoglobulins of the IgM, IgG_1, IgG_{2a}, IgG_{2b}, IgG_3 and IgA isotypes in wild-type and C2GnT2-deficient mice is graphed. Data shown is pooled from two separate experiments, each of at least 5 mice of each genotype per an experiment. (b) Mean mucosal IgA levels in wild-type and C2GnT2-deficient mice fecal samples is graphed. All values are means ± S.E.M. (*$p<0.05$)

Figure 6

Behavior and thyroid function in C2GnT3-deficient mice

(a) Results from the tube test for social dominance are graphed. The results shown are representative of three separate experiments. (b) Mean circulating T4 levels in wild-type and C2GnT3-deficient mice is graphed. (c) Mean circulating T4 levels in wild-type and C2GnT3-deficient mice following diet supplementation with 0.025% thyroid powder for 2 weeks is shown. (d) Outcome of social dominance assay performed with wild-type and C2GnT3-deficient

mice treated with 0.025% thyroid powder supplemented chow is shown. (e) Mean circulating levels of the TSH in wild-type and C2GnT3-deficient mice is graphed. (f) Average amount by which TRH stimulation increased T4 in circulation after 1 and 2 hours in wild-type and C2GnT3-deficient mice is shown. (g) The mean relative amount of biotinylated T4 remaining at each time point is graphed. All capped and uncapped error bars represent S.E.M. (*$p<0.05$; **$p<0.01$)

Figure 7

Enzyme activity in tissue lysates from mice deficient for C2GnTs

(a) Relative C2GnT and C4GnT activity in tissue lysates from C2GnT2-deficient mice is graphed. (b and c) C2GnT activity in tissue lysates from (b) C2GnT3-deficient and (c) triply deficient mice relative to activity in wild-type control tissues is shown. Values represent means ± S.E.M. (*$p<0.05$, ***$p<0.001$)

Table I. O-glycan structures in the presence and absence of C2GnTs

Structural characteristics	Examples of structure		Changes relative to WT		
			C2GnT2$^{\Delta/\Delta}$	C2GnT3$^{\Delta/\Delta}$	T1/T2/T3
Stomach					
Core 2		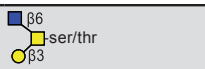	↓↓	=	ND
Elongated Core 1	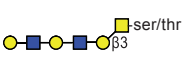	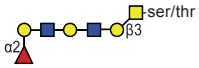	↑↑	=	↑↑↑
I- Branches		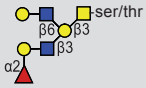	↓↓	=	ND
Elongated O-mannose	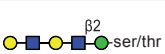	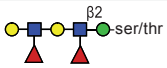	↑	=	↑↑↑
Colon					
Core 2	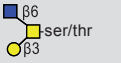	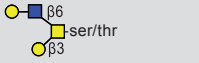	↓↓	=	ND
Elongated Core 1	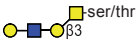	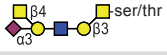	↑↑	=	↑↑↑
I- Branches			↓↓↓	=	ND
Small Intestine					
Core 2		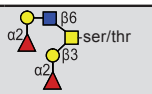	↓	↓↓	ND
Core 1 & Elongated Core 1	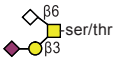	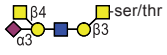	↑	↑↑	↑↑↑
Kidneys					
Core 2	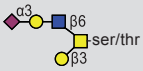		=	=	ND
Core 1 & Elongated Core 1	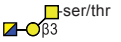	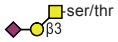	=	=	=
Thyroid / Trachea					
Core 2	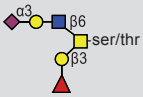		NA	↓	NA
Core 1 & Elongated Core 1	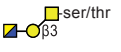	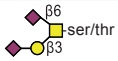	NA	↑	NA
Sd^a	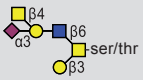	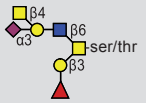	NA	↓	NA
Thymus					
Core 2	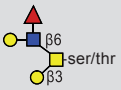		NA	=	NA
Core 1 & Elongated Core 1	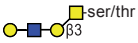	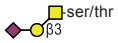	NA	=	NA

The structural changes described here are based on MALDI-TOF/TOF MS and MS/MS data. WT, wild-type mice; C2GnT2$^{\Delta/\Delta}$, C2GnT2-deficient mice; C2GnT3$^{\Delta/\Delta}$, C2GnT3-deficient mice; T1/T2/T3, C2GnT triple-deficient mice; NA, not analysed; ND, none detected; =, no significant changes; ser, serine; thr, threonine; upward arrows represent increase; downward arrows represent decrease; the number of arrows is indicative of the magnitude of change with 3 arrows being the greatest (>75%) and 1 arrow the smallest (<25%) percent of change from wild type. Linkages are assigned according to the biosynthetic pathways known. □, *N*-acetylgalactosamine (GalNAc); ■, *N*-acetylglucosamine (GlcNAc); ◪, GalNAc or GlcNAc; ○, galactose; ●, mannose; ◆, *N*-acetylneuraminic acid; ◇, *N*-glycolylneuraminic acid; ▲, fucose.

Figure 1

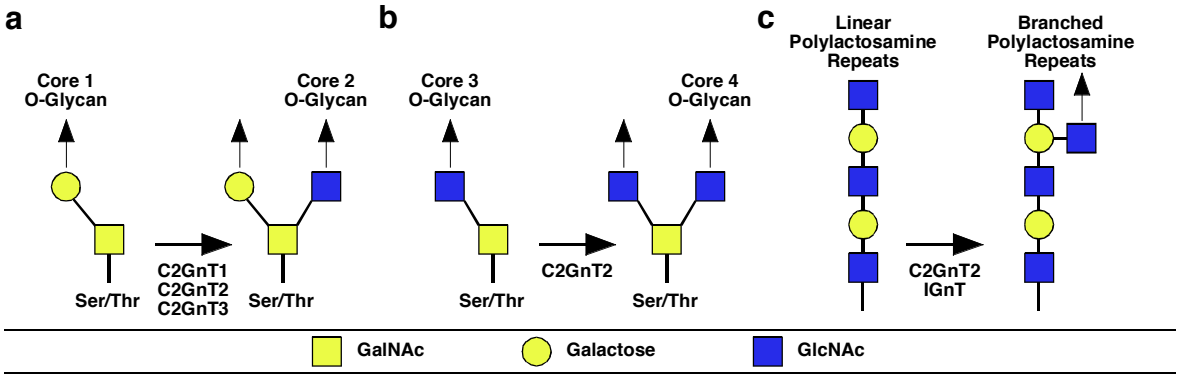
a
Core 1
O-Glycan
Ser/Thr
C2GnT1
C2GnT2
C2GnT3
Core 2
O-Glycan
Ser/Thr
b
Core 3
O-Glycan
Ser/Thr
C2GnT2
Core 4
O-Glycan
Ser/Thr
c
Linear
Polylactosamine
Repeats
C2GnT2
IGnT
Branched
Polylactosamine
Repeats
GalNAc
Galactose
GlcNAc

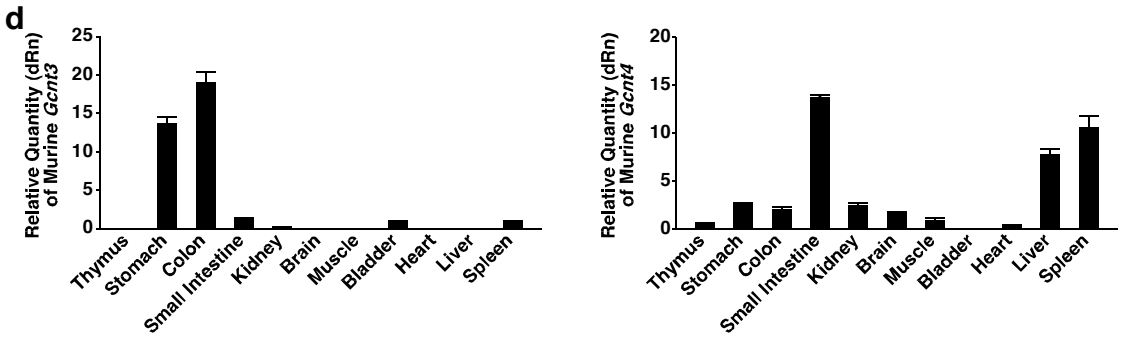
d
Relative Quantity (dRn)
of Murine Gcnt3
25
20
15
10
5
0
Thymus
Stomach
Colon
Small Intestine
Kidney
Brain
Muscle
Bladder
Heart
Liver
Spleen
Relative Quantity (dRn)
of Murine Gcnt4
20
15
10
5
0
Thymus
Stomach
Colon
Small Intestine
Kidney
Brain
Muscle
Bladder
Heart
Liver
Spleen

Figure 2

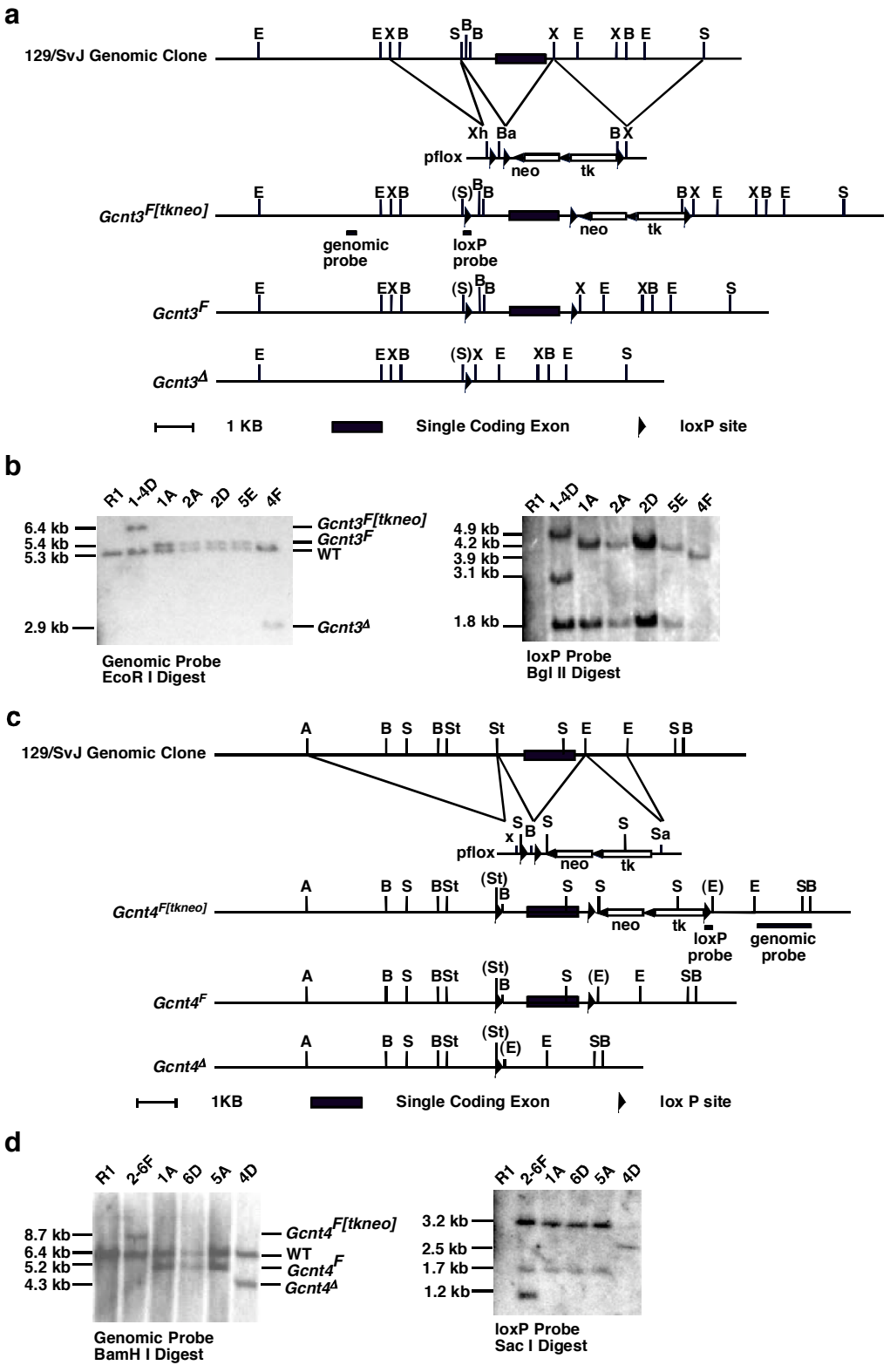
a
129/SvJ Genomic Clone
pflox
neo
tk
Gcnt3F[tkneo]
genomic probe
loxP probe
Gcnt3F
Gcnt3Δ
1 KB
Single Coding Exon
loxP site
b
6.4 kb
5.4 kb
5.3 kb
2.9 kb
Gcnt3F[tkneo]
Gcnt3F
WT
Gcnt3Δ
Genomic Probe
EcoR I Digest
4.9 kb
4.2 kb
3.9 kb
3.1 kb
1.8 kb
loxP Probe
Bgl II Digest
c
129/SvJ Genomic Clone
Gcnt4F[tkneo]
Gcnt4F
Gcnt4Δ
1KB
Single Coding Exon
lox P site
d
8.7 kb
6.4 kb
5.2 kb
4.3 kb
Genomic Probe
BamH I Digest
3.2 kb
2.5 kb
1.7 kb
1.2 kb
loxP Probe
Sac I Digest

Figure 3

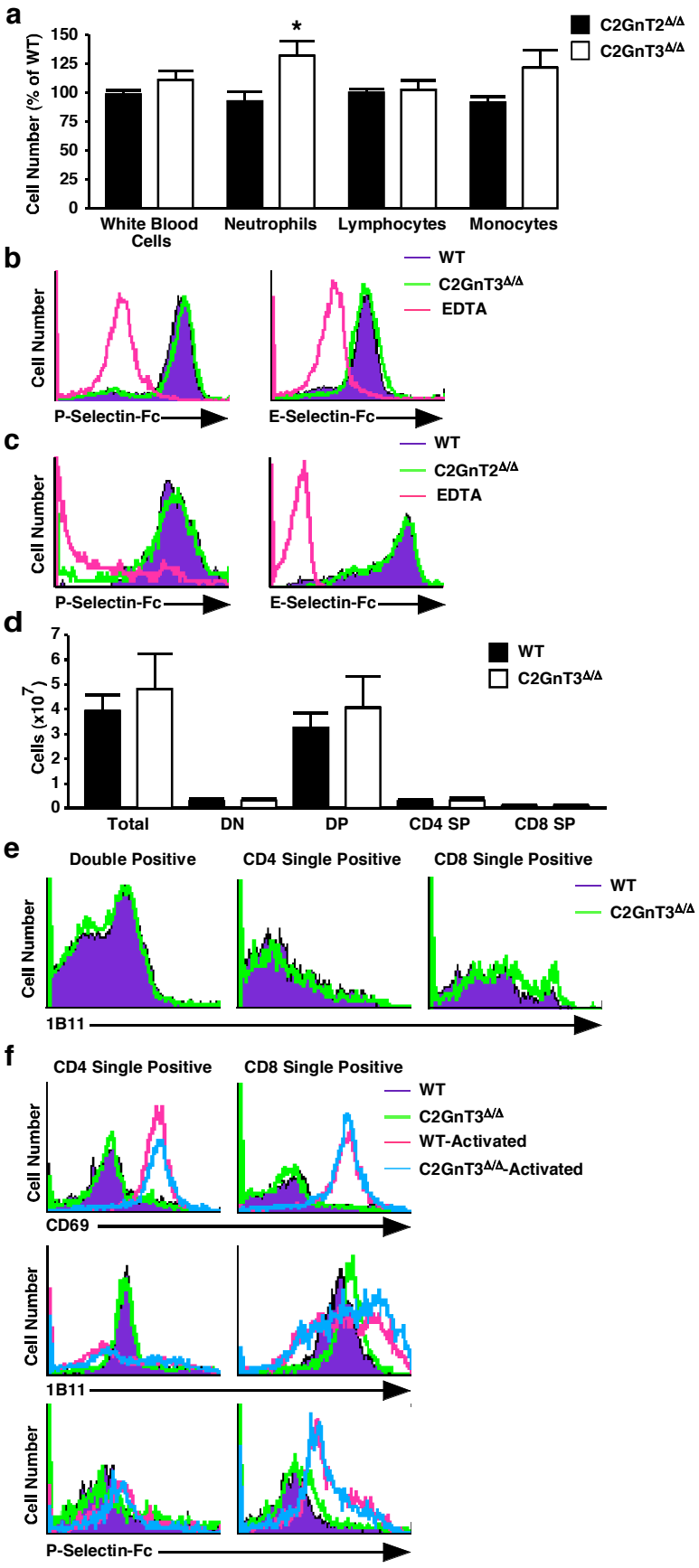
a
Cell Number (% of WT)
150
125
100
75
50
25
0
*
C2GnT2Δ/Δ
C2GnT3Δ/Δ
White Blood Cells
Neutrophils
Lymphocytes
Monocytes
b
Cell Number
WT
C2GnT3Δ/Δ
EDTA
P-Selectin-Fc
E-Selectin-Fc
c
Cell Number
WT
C2GnT2Δ/Δ
EDTA
P-Selectin-Fc
E-Selectin-Fc
d
Cells (x10^7)
7
6
5
4
3
2
1
0
WT
C2GnT3Δ/Δ
Total
DN
DP
CD4 SP
CD8 SP
e
Double Positive
CD4 Single Positive
CD8 Single Positive
Cell Number
WT
C2GnT3Δ/Δ
1B11
f
CD4 Single Positive
CD8 Single Positive
Cell Number
WT
C2GnT3Δ/Δ
WT-Activated
C2GnT3Δ/Δ-Activated
CD69
Cell Number
1B11
Cell Number
P-Selectin-Fc

Figure 4

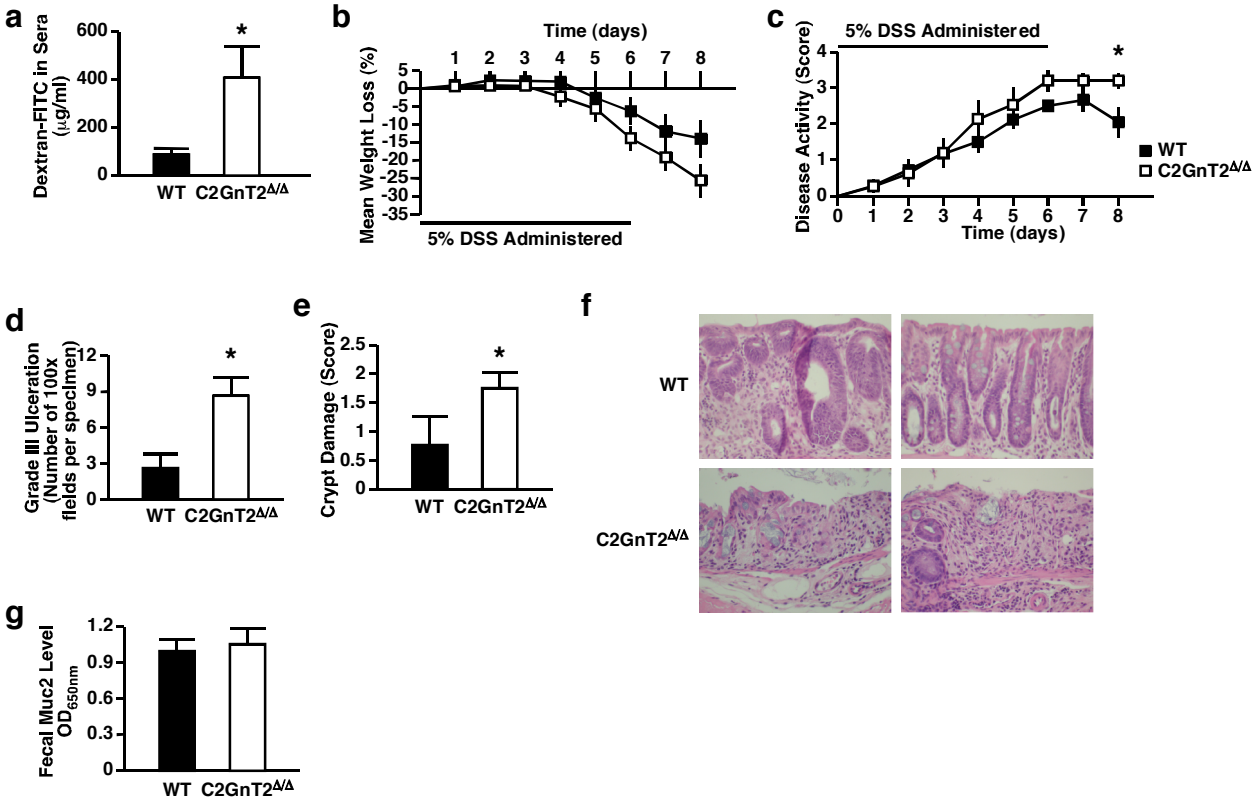
a
Dextran-FITC in Sera (μg/ml)
600
400
200
0
*
WT C2GnT2Δ/Δ
b
Time (days)
1 2 3 4 5 6 7 8
Mean Weight Loss (%)
5 0 -5 -10 -15 -20 -25 -30 -35
5% DSS Administered
c
5% DSS Administered
Disease Activity (Score)
4 3 2 1 0
*
0 1 2 3 4 5 6 7 8
Time (days)
WT
C2GnT2Δ/Δ
d
Grade III Ulceration (Number of 100x fields per specimen)
12 9 6 3 0
*
WT C2GnT2Δ/Δ
e
Crypt Damage (Score)
2.5 2 1.5 1 0.5 0
*
WT C2GnT2Δ/Δ
f
WT
C2GnT2Δ/Δ
g
Fecal Muc2 Level OD650nm
1.2 0.9 0.6 0.3 0
WT C2GnT2Δ/Δ

Figure 5

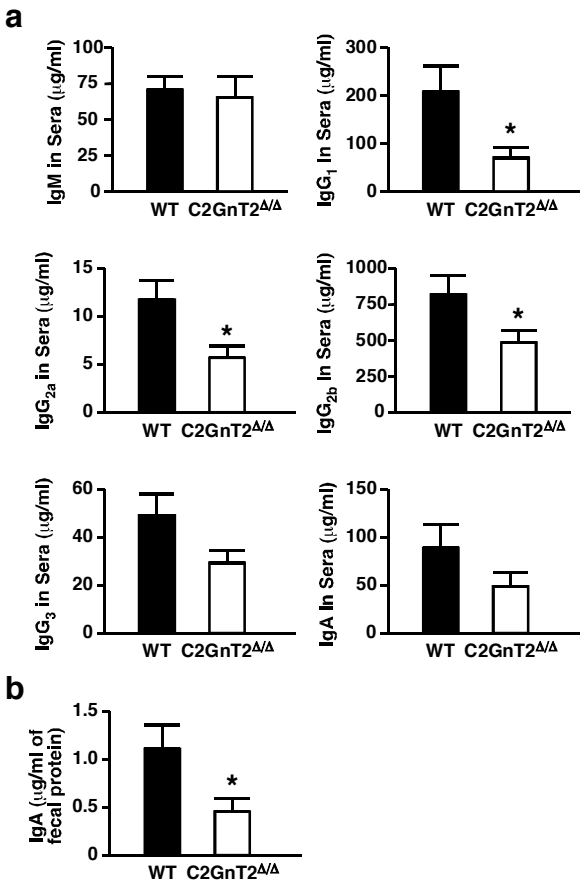
a
IgM in Sera (μg/ml)
100
75
50
25
0
WT C2GnT2Δ/Δ
IgG1 In Sera (μg/ml)
300
200
100
0
*
IgG2a in Sera (μg/ml)
15
10
5
IgG2b In Sera (μg/ml)
1000
750
500
250
IgG3 in Sera (μg/ml)
60
40
20
IgA In Sera (μg/ml)
150
b
IgA (μg/ml of fecal protein)
1.5
1.0
0.5

Figure 6

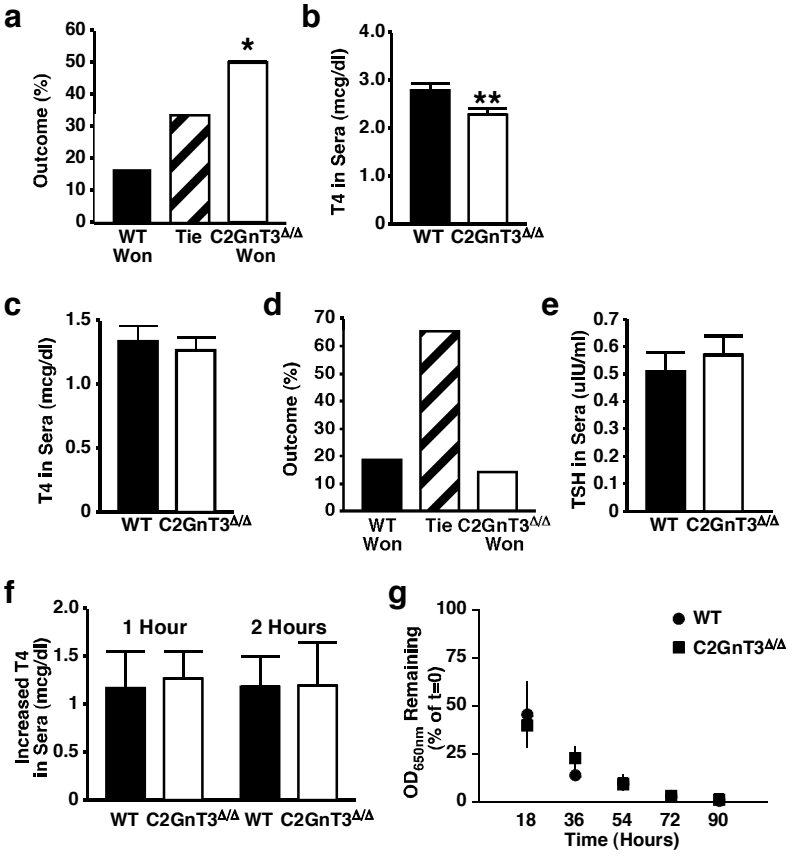
a
Outcome (%)
60
50
40
30
20
10
0
*
WT Won
Tie
C2GnT3Δ/Δ Won
b
T4 in Sera (mcg/dl)
4.0
3.0
2.0
1.0
0
**
WT
C2GnT3Δ/Δ
c
T4 in Sera (mcg/dl)
1.5
1.0
0.5
0
WT
C2GnT3Δ/Δ
d
Outcome (%)
70
60
50
40
30
20
10
0
WT Won
Tie
C2GnT3Δ/Δ Won
e
TSH in Sera (uIU/ml)
0.7
0.6
0.5
0.4
0.3
0.2
0.1
0
WT
C2GnT3Δ/Δ
f
Increased T4 in Sera (mcg/dl)
2.0
1.5
1
0.5
0
1 Hour
2 Hours
WT
C2GnT3Δ/Δ
WT
C2GnT3Δ/Δ
g
OD650nm Remaining (% of t=0)
100
75
50
25
0
WT
C2GnT3Δ/Δ
18
36
54
72
90
Time (Hours)

Figure 7

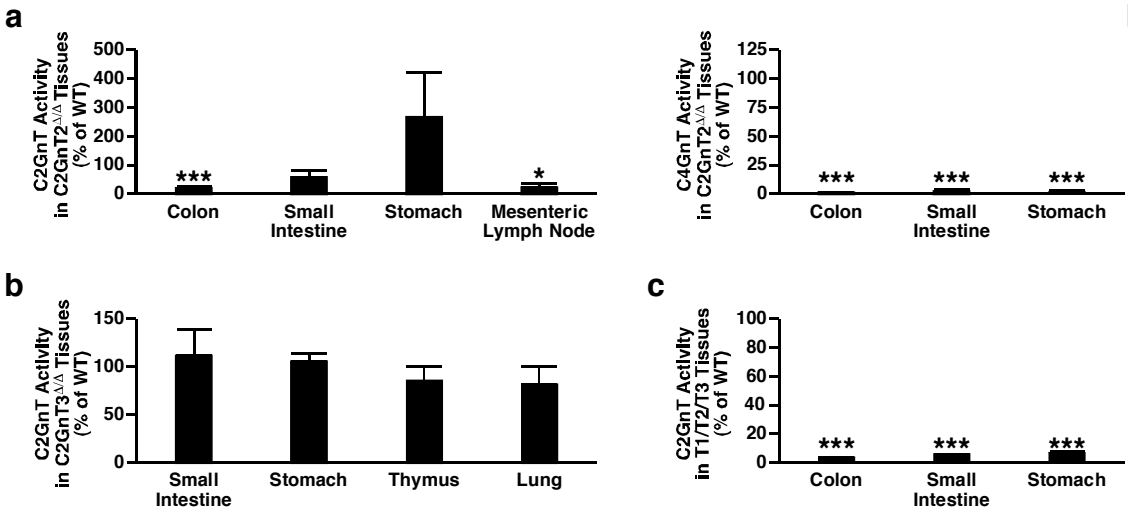
a
C2GnT Activity in C2GnT2Δ/Δ Tissues (% of WT)
500
400
300
200
100
0
***
*
Colon
Small Intestine
Stomach
Mesenteric Lymph Node
C4GnT Activity in C2GnT2Δ/Δ Tissues (% of WT)
125
100
75
50
25
0
***
***
***
Colon
Small Intestine
Stomach
b
C2GnT Activity in C2GnT3Δ/Δ Tissues (% of WT)
150
100
50
0
Small Intestine
Stomach
Thymus
Lung
c
C2GnT Activity in T1/T2/T3 Tissues (% of WT)
100
80
60
40
20
0
***
***
***
Colon
Small Intestine
Stomach